

# Improved estimation of aerosol optical depth from MODIS imagery over land surfaces

Shunlin Liang<sup>\*</sup>, Bo Zhong, Hongliang Fang

*Department of Geography, University of Maryland, College Park, MD 20742, USA*

Received 11 October 2005; received in revised form 9 May 2006; accepted 25 May 2006

## Abstract

Estimation of aerosol loadings is of great importance to the studies on global climate changes. The current Moderate-Resolution Imaging Spectroradiometer (MODIS) aerosol estimation algorithm over land is based on the “dark-object” approach, which works only over densely vegetated (“dark”) surfaces. In this study, we develop a new aerosol estimation algorithm that uses the temporal signatures from a sequence of MODIS imagery over land surfaces, particularly “bright” surfaces. The estimated aerosol optical depth is validated by Aerosol Robotic Network (AERONET) measurements. Case studies indicate that this algorithm can retrieve aerosol optical depths reasonably well from the winter MODIS imagery at seven sites: four sites in the greater Washington, DC area, USA; Beijing City, China; Banizoumbou, Niger, Africa; and Bratts Lake, Canada. The MODIS aerosol estimation algorithm over land (MOD04), however, does not perform well over these non-vegetated surfaces. This new algorithm has the potential to be used for other satellite images that have similar temporal resolutions.

© 2006 Elsevier Inc. All rights reserved.

*Keywords:* Aerosol; MODIS; Remote sensing; Land surfaces

## 1. Introduction

Atmospheric aerosol plays a significant role in the Earth’s radiation budget through radiative forcing and chemical perturbations. Anthropogenic aerosols are intricately linked to the climate system and the hydrologic cycle. The net effect of aerosols is to cool the climate system by reflecting sunlight (Kaufman et al., 2002). Quantifying the net effect requires accurate information on the global distribution of aerosol properties that have to be estimated from satellite observations. Estimating aerosol properties is also one of the first steps in generating high-level land surface products from satellite observations.

The Moderate-Resolution Imaging Spectroradiometer (MODIS) is one of the sensors in the NASA Earth observing system (EOS) Terra platform launched on December 18, 1999 for imaging in the morning, and the Aqua platform launched on May 4, 2002 for imaging on the afternoon. MODIS has 36 spectral bands spanning from the visible to the thermal-infrared

(IR) spectrum. The spatial resolution varies from 250 m (bands 1 and 2), 500 m (bands 3–7), to 1000 m (bands 8–36). The swath width of MODIS is about 2300 km, with the across-track field-of-view angle of 110°. Each MODIS has the global coverage every 2 days, with a 1-day or more frequent repeat at higher latitudes greater than 30° due to orbital convergence. The details of the sensor characterization are available elsewhere (Salomonson et al., 1989).

There is a relatively long history of the quantitative estimation of aerosol optical depth from remotely sensed imagery (Liang, 2004), for example, using multiangular information (Diner et al., 2005; North, 2002), polarization information (Deuze et al., 2001), multispectral information (Kaufman et al., 1997b; Liang & Fang, 2004; Liang et al., 1997; Teillet & Fedosejevs, 1995) and multitemporal information (Christopher et al., 2002; Hauser et al., 2005; Zhang & Christopher, 2001). The MODIS science team (Kaufman et al., 1997a, 1997b; Remer et al., 2005) uses the dark-object method to estimate aerosol optical depth from MODIS imagery over land for climate study. However, its major limitation is its suitability only for densely vegetated (“dark”) surfaces. If no dense vegetation canopies are detected in the window of 10 km

<sup>\*</sup> Corresponding author. Tel.: +1 301 405 4556; fax: +1 301 314 9299.  
E-mail address: [sliang@umd.edu](mailto:sliang@umd.edu) (S. Liang).

by 10km, no aerosol retrieval occurs. The recent validation results of the MODIS aerosol optical depth (e.g., Levy et al., 2005; Tripathi et al., 2005) indicate the need for improvement.

There are few alternative algorithms (e.g., Hsu et al., 2004; Tang et al., 2005). For example, Hsu et al. (2004) proposes a new approach to retrieve aerosol properties over bright surfaces using the minimum reflectance determined from  $0.1^\circ \times 0.1^\circ$  grid. The spatial resolution is not sufficient for atmospheric correction of MODIS imagery at 500m or 1km scale. The accuracy of 30% at this scale also needs to be improved. Tang et al. (2005) establishes an empirical relationship between the top-of-atmosphere reflectance and surface reflectance, and MODIS data from two successive orbits are used to solve the nonlinear equation. Any errors resulting from geometric registration and subpixel clouds may significantly affect the solutions. Therefore, further development of new algorithms is critically needed, particularly for bright surfaces.

In this study, we develop a new algorithm for estimating the aerosol optical depths using multi-temporal MODIS data over land surfaces. This algorithm is validated using AERONET measurements. The rest of this paper will start with a brief overview of the official MODIS algorithm, and then describe a new algorithm. Case studies are presented in Section 4 to validate and demonstrate this new algorithm. A short summary and some remaining issues are discussed in the last section.

## 2. The MODIS algorithm

In the past decade, the MODIS team has developed the “dark-object” method for aerosol estimation (Kaufman et al., 1997a, 1997b; Kaufman et al., 2000). The “dark-object” method is probably the most widely used approach for atmospherically correcting different remotely sensed imagery (Kaufman et al., 1997a; Kaufman et al., 2000; Liang et al., 1997; Popp, 1995; Teillet & Fedosejevs, 1995). The basic assumption is that if the surface is densely vegetated, the middle infrared surface reflectances around  $2.1\mu\text{m}$  (MODIS band 7)  $\rho_7$  are linearly related to surface reflectances at the blue band (band 3 around  $0.49\mu\text{m}$ )  $\rho_3$  and the red band (band 1 around  $0.66\mu\text{m}$ )  $\rho_1$ . Since most aerosol sizes are smaller than the middle-IR wavelength, aerosol effects in band 7 are negligible and its surface reflectance ( $\rho_7$ ) can then be easily estimated. Based on surface measurements, Kaufman et al. (1997b) established the following empirical formulae:

$$\begin{cases} \rho_1/\rho_7 = 0.25 \\ \rho_3/\rho_7 = 0.5 \end{cases} \quad (1)$$

After calculating surface reflectances of bands 3 and 1 ( $\rho_1$ ,  $\rho_3$ ) from their linear relationships with band 7 reflectance ( $\rho_7$ ), aerosol optical depths at bands 1 and 3 can be estimated by using the look-up tables. These look-up tables are pre-calculated for each aerosol models that are pre-defined for a given location and time.

There are two key requirements associated with this method: (1) existence of large homogeneous dense vegetation in the scene; (2) stable empirical relationships of surface reflectance

between band 7 and bands 3 and 1. The first requirement precludes the accurate reflectance retrieval of surfaces with non-dense vegetation canopies. To meet the second requirement, dense vegetation canopies have to be distinguished from other dark objects, such as wet soil and water.

If no dense vegetation canopies are detected in the window of 10km by 10km, no aerosol retrieval occurs. As a result, the spatial distribution of the aerosol optical depth from the MODIS algorithm (MOD04) has the chessboard-like pattern, where some windows are based on the actual retrievals, and others are filled. MODIS surface reflectance product (MOD09) uses the similar algorithm to derive aerosol optical depth for atmospheric correction. For non-dense vegetation surfaces (e.g., snow/ice, desert, agricultural lands before and after the growing peak), MOD09 products are not accurate because of no aerosol correction with the actual retrieval, which results in large errors in the downstream products, such as snow/desert albedo and canopy leaf area index. After examining the MODIS aerosol optical depth product around the world, it is found that in many cases (mainly off growing season) the MODIS algorithm fails to retrieve aerosol optical depth over land because the surfaces are not covered by dense vegetation canopies. In a particular example, after obtaining 99 MOD04 files from U. S. Geological Service (USGS) EROS Data Center (EDC) over the greater Washington, DC area, centered at Goddard Space Flight Center, after specifying the order for year 2001, there were only 29 actual aerosol retrievals out of 99, which leads to less than 30%.

## 3. The new algorithm

The new aerosol estimation algorithm over land takes full advantage of MODIS multitemporal observation capability, particularly when we combine observations from both Terra and Aqua platforms. The flow chart of the algorithm is shown in Fig. 1. The central idea of this algorithm is to detect the “clearest” observation during a temporal window for each pixel. If we assume the aerosol optical depths for the “clearest” observations to be known, the aerosol optical depths of other “hazy” observations can be interpolated from the surface reflectance of the “clearest” observations.

We will follow the current MODIS aerosol estimation algorithm (Kaufman et al., 1997a, 1997b; Remer et al., 2005) as much as possible so that we can take full advantage of whatever has been developed for operational applications. The major differences are discussed as follows.

(1) Identifying the “clearest” observations of each pixel and converting their TOA reflectance to surface reflectance. MODIS has acquired data since the year 2000. The multi-temporal observations are used to determine the “clearest” observations. The “clearest” one corresponds to the minimal aerosol contamination, thus, the surface reflectance can be determined with less uncertainty. The idea has been used to determine surface reflectance from other sensors, such as Missions of the Total Ozone Mapping Spectrometer (TOMS) (Hapke, 1984; Herman et al., 2001) and Geostationary Operational Environmental Satellite (GOES) (Christopher et al., 2002; Wang et al., 2003).

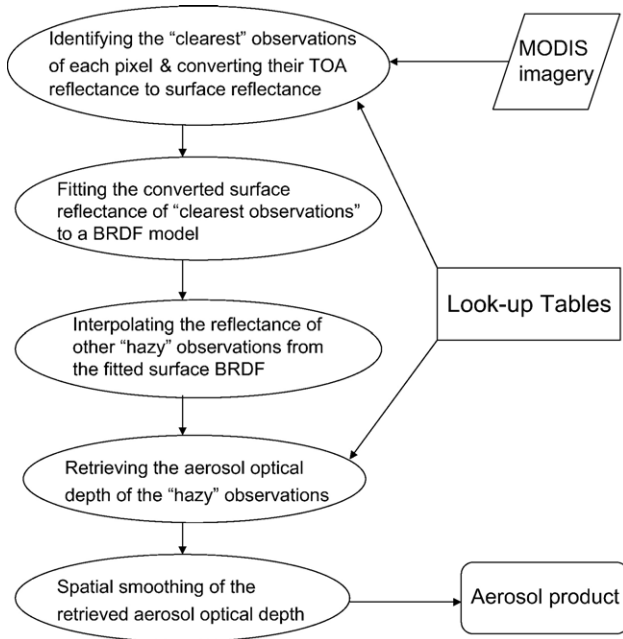


Fig. 1. Flow chart of this new algorithm for estimating aerosol optical depth from MODIS data.

In a temporal window, we assume that there may be  $N$  clear-sky observations. Although other techniques might be useful, the minimum blue band (band 3) apparent reflectance has been successfully used to determine these “clearest” observations in our experiments, since aerosol scattering increases blue radiance significantly. It is realized through a look-up table procedure. For each aerosol type, there is one table including atmospheric visibility, aerosol optical depth, atmospheric optical parameters (e.g., path radiance, transmittance) and angular information. The visibility value is used for table searching, but it has the unique correspondence with the aerosol optical depth. The reason for using visibility simply reflects the fact that it is one of the inputs to MODTRAN that is used for this study. A constant aerosol optical depth value (corresponding to 100km visibility value) is set for the clearest sky condition, thus, top-of-atmosphere (TOA) radiance of all clear-sky observations are converted to surface reflectance through the look-up table method. Although the aerosol optical depth value is assumed to be the same, different sun-viewing geometries have been accounted for so that all optical parameters of the atmosphere (e.g., path radiance, spherical albedo, transmittance) are variable. As shown in Fig. 2, 0.07 at 440nm seems a very reasonable value for the clearest

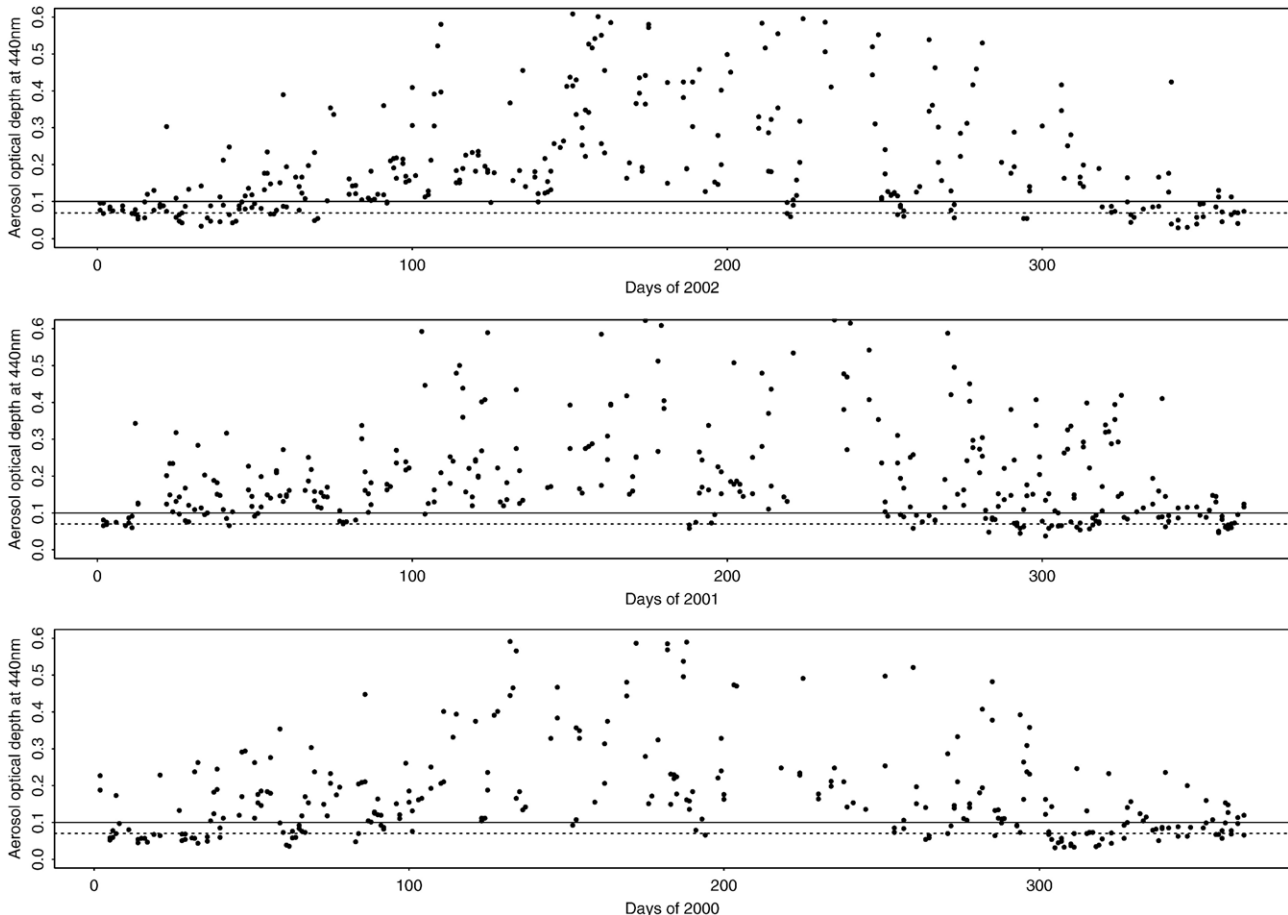


Fig. 2. The observed aerosol optical depths at 440nm ( $\tau_{440}$ ) from AERONET located at the NASA Goddard Space Flight Center during the last 3 years (2000–2002) with Terra and Aqua overpasses. Dashed lines represent aerosol optical depth equals 0.07.

atmospheric condition as in the greater Washington, DC area (see the discussions in the section of case studies from Fig. 2). It appears that its value needs to vary spatially. For the global implementation, it can be determined based on the aerosol climatologies that may be done from multiple sources, such as AERONET observations (Holben et al., 1998), TOMS aerosol climatology (Torres et al., 2002), Multi-angle Imaging Spectro-radiometer (MISR) retrievals (Martonchik et al., 1998, 2002), MODIS retrievals, and so on. Since the value in each band is so small, the uncertainty will not cause a significant impact.

Determining the length of the temporal window needs to be done carefully. Obviously, it needs to be short enough so that the surface properties do not change dramatically but long enough to include adequate clearest observations. In all our case studies (Section 4), it seems a 3-month period is a reasonable choice.

To avoid selecting a cloud-shadowing observation, we may use the MODIS cloud products. It is found, however, that the upwelling TOA radiance of a cloud-shadowing observation is usually smaller than the path radiance of a predefined clear atmosphere, since there is no direct solar illumination in the field of view. These cloud-shadowing observations are labeled when their converted surface reflectances are negative. In general, shadows look much more obvious in the near-IR bands than in the visible bands because multiple scattering dominates in the visible bands and therefore reduces the shadowing effects significantly.

(2) Fitting the converted surface reflectance of “clearest observations” to a statistical model that combines the bidirectional reflectance distribution function (BRDF) kernel and a temporal kernel (Liang & Townshend, 1997). The Walthall model (Walthall et al., 1985) is used for the BRDF kernel and the low-order Fourier function for the temporal kernel. As long as the “clearest” observations are identified, other observations in the working temporal window are treated as “hazy” observations.

(3) Interpolating the reflectance of other “hazy” observations from the fitted surface temporal BRDF in step 1 above within this temporal window. If the temporal window is short enough, surface reflectance can be assumed to be constant. However, surface reflectance of the “hazy” observations are interpolated from the “clearest” observations to account for the possible variations in surface reflectance within the temporal window.

Note that the near-IR bands are rarely contaminated by aerosol scattering if the aerosol particles are small (e.g., biomass burning, industrial pollutants) and only gaseous absorption is considered in determining their surface reflectances at this point. As long as an equation for each band is established from the “clearest” observations, the near-IR reflectances of other “hazy” observations could be used to predict the surface reflectance of these visible bands. This idea was used in the atmospheric correction algorithm for Enhanced Thematic Mapper Plus (ETM+) data (Liang et al., 2001; Liang & Fang, 2004) and all the “dark-object” methods (Kaufman et al., 1997a, 1997b; Liang et al., 1997; Teillet & Fedosejevs, 1995). However, it is found that in many cases near-IR bands are

also contaminated by aerosols (e.g., desert dust aerosols of which the radius is typically larger than  $1\ \mu\text{m}$ , and have high aerosol optical depth even in the near-IR bands), experiments in this study show that this approach does not work as well as expected.

(4) Retrieving the aerosol optical depth of the “hazy” observations in each visible band by searching the look-up tables based on the TOA radiance and surface reflectance. If the surface is assumed to be Lambertian, an analytic formula is available to link TOA radiance with surface reflectance (Liang, 2004). For a non-Lambertian surface, Qin et al. (2001) derive a matrix expression of TOA radiance for coupling surface BRDF without using any simplifications. Experiments in this study indicate that the assumption of Lambertian is adequate for the blue band and in the case studies later we simply used a linear interpolation.

(5) Spatial smoothing of the retrieved aerosol optical depth. The aerosol optical depth is estimated on the pixel basis in the previous steps. Common knowledge indicates that the spatial variation of aerosol optical depth is much smoother than the surface features. In the current MODIS product, an average value is calculated for each window of  $10\text{ km} \times 10\text{ km}$ . In the MISR aerosol product, the window size is  $17.6\text{ km} \times 17.6\text{ km}$ . A spatial smoothing process is necessary in our new algorithm based on the estimates from  $1\text{ km}$  pixels, which can also reduce the uncertainty possibly introduced by various approximations in the previous steps. The “smart-smoothing” technique developed before (Fallah-Adl et al., 1997) is suitable here.

In fact, this new algorithm has its heritage because the similar idea has been successfully explored in the First ISLSCP Field Experiments (FIFE) Thematic Mapper (TM) imagery processing (Hall et al., 1991) and also used by others (e.g., Chavez, 1996; Moran et al., 1992) in simplified ways. The similar idea was used by the land remote sensing community for many years, starting with the maximum normalized difference vegetation index (NDVI) compositing scheme (Holben, 1986). However, the maximum NDVI does not correspond to the minimum aerosol scattering, particularly over non-vegetated surfaces. The compositing schemes neither produce aerosol optical depth and surface reflectances nor consider spatial dependence.

#### 4. Case studies

To validate the new algorithm, this study analyzes AERONET measurements (Holben et al., 1998) and implements this algorithm using MODIS  $1\text{ km}$  data at four test sites. For all sites the rural aerosol model (MODTRAN default) is used, except the Africa site where the dust aerosol model (Kaufman et al., 1997c) is used. The retrieved aerosol optical depths from the blue band (band 3) are compared with AERONET measurements. In this process, MODIS 1B data are first transferred using the map projection tool. The values of the pixel corresponding to the AERONET site are then extracted and the aerosol optical depth values are estimated using the new algorithm. The AERONET measurements closest to the satellite

overpass (all are within the temporal window of 20 min) are used to compare with the retrieved. So each point in the figures (Figs. 2–9) represents the match at a specific location

(AERONET site) and a specific time (closest to satellite overpass). The validation results are characterized by both residual standard error and multiple  $R$ -squared ( $R^2$ ) value,

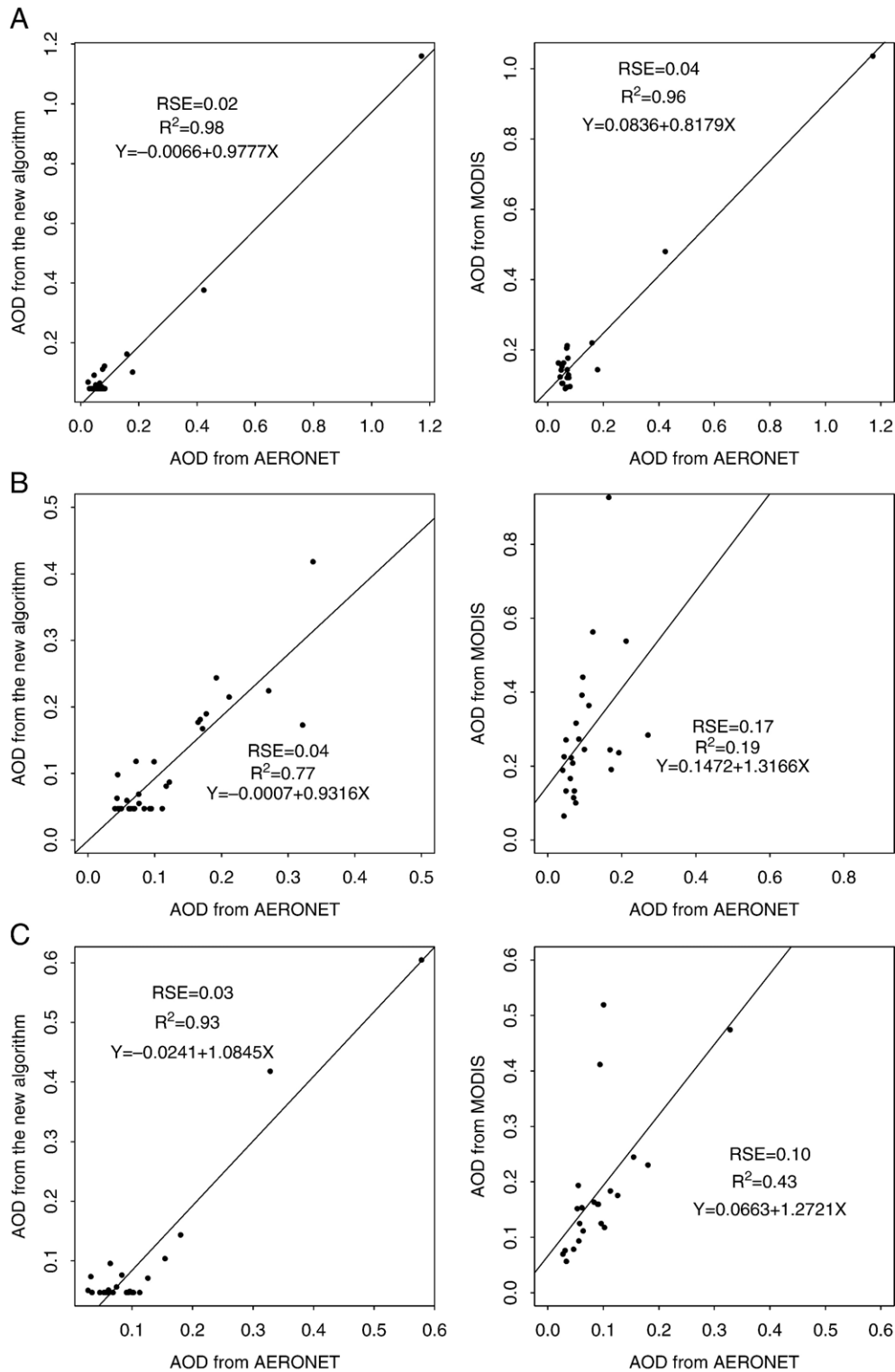


Fig. 3. Validation results using the AERONET measurements over the greater Washington, DC region at four sites: GSFC (A), MD Science Center (B), SERC (C), and Wallops (D). The aerosol optical depth (AOD) corresponds to MODIS blue band (band 3). For each site, the left plot is for validating the new algorithm and the right plot is for the MOD04 product. Note the solid line is the regression line and the regression equation ( $Y$  stands for  $y$ -axis and  $X$  for  $x$ -axis) is also given in each plot.

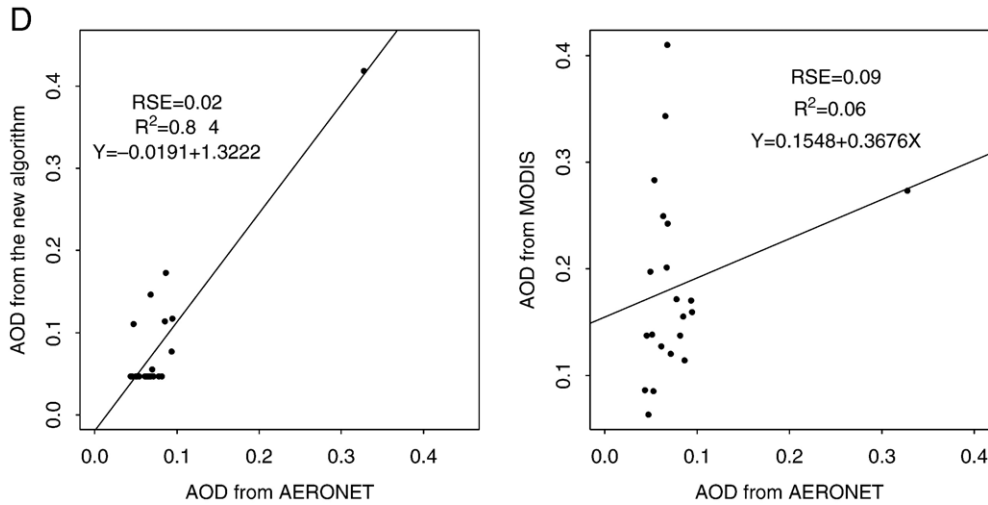


Fig. 3 (continued).

which are provided by almost all statistical software packages for linear regression analysis.

Note that the atmosphere tends to be more cloudy and hazy over most vegetated surfaces, which is usually during the growing season or in a humid environment. In this case, the MODIS “dark-object” method is expected to do a reasonable job. The atmosphere over bright surfaces tends to have clear days more frequently and surface properties tend to be more stable. Thus, the proposed new algorithm will be more effective. It is not, of course, always true. For example, the aerosol optical depth over the Amazon basin is very low (about 0.10 in the visible region) for about 8 months each year due to low aerosol production and large wet removal from rainfall, while the aerosol of depth over the Sahara is high at all times due to desert dust aerosols. Although this proposed new algorithm is theoretically suitable for all surfaces, it

might be best to combine it with the current MODIS “dark-object” method.

Fig. 2 shows the observed aerosol optical depths at 440 nm ( $\tau_{440}$ ) from AERONET over the NASA Goddard Space Flight Center (GSFC) (39.03°N, 76.88°W) in the last 3 years (2000–2002) with Terra and Aqua overpasses. Note that observations with optical depth larger than 0.6 are filtered out from these plots. The solid and dashed lines are for  $\tau_{440}=0.1$  and  $\tau_{440}=0.07$ . When  $\tau_{440} \leq 0.1$ , the imagery usually looks very clear.

Several critical points can be observed from this figure. First, there are so many clear days before (around early April) and after (around October) the growing season that enable us to implement the algorithm extremely well. Second, the threshold value ( $\tau_{440}=0.07$ ) characterizes the clear days reasonably well. Third, there are tremendous amounts of

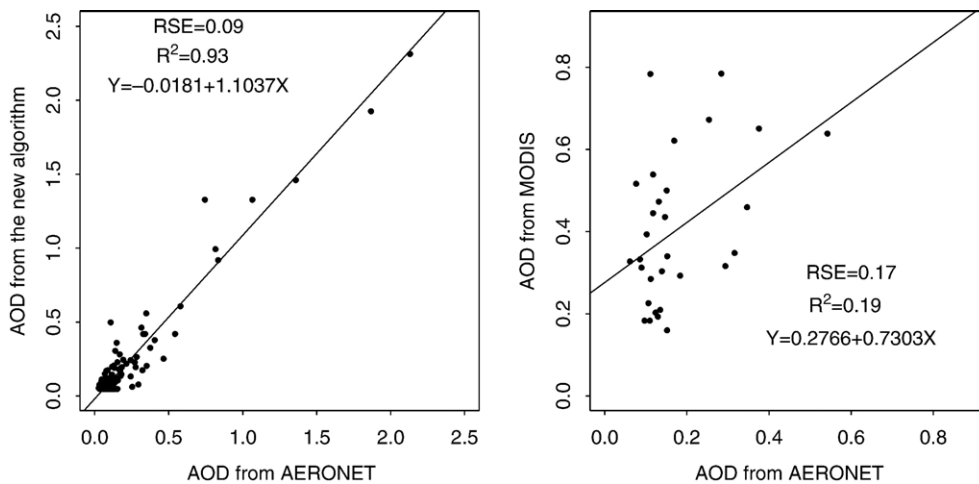


Fig. 4. Validation results using AERONET measurements at Beijing City, China. Like Fig. 3, the left plot is for validating the new algorithm and the right plot is for the MOD04 product. The solid line is the regression line and the regression equation is also given in each plot. The aerosol optical thickness (AOT) corresponds to MODIS blue band (band 3).

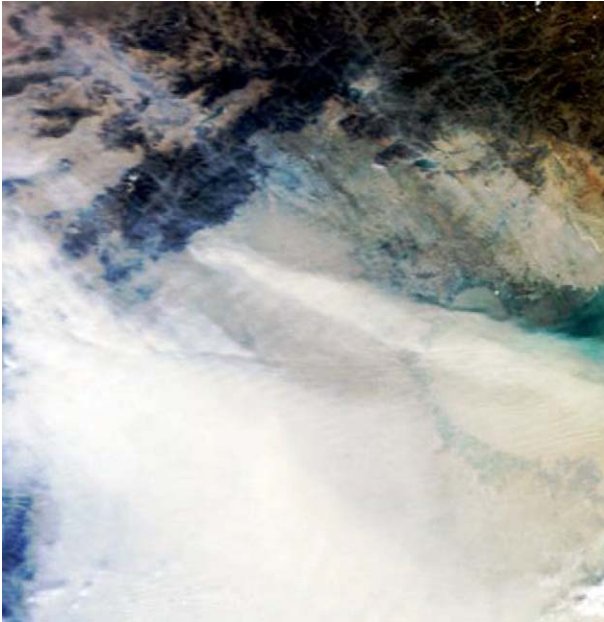


Fig. 5. The true-color composite image of MODIS imagery (bands 1, 3 and 4) over the Beijing area, China, acquired on November 11, 2002. The spatial resolution is 1 km.

variations in aerosol optical depth before and after the growing season when the MODIS “dark-object” method completely fails, which can lead to significant uncertainty in the downstream land surface products. Last, while there is less frequency of clear images during the growing season in this geographic region, the “dark-object” algorithm will be expected to work well. So it will be best to estimate the complete aerosol dynamics in both space and time if the new algorithm is used as a complementary algorithm to the current MODIS “dark-object” method.

In the first case, 396 MODIS images over the greater Washington, DC area from September 1, 2002 to April 1, 2003 were downloaded. During this time, surfaces are mostly non-vegetated. After converting blue band (band 3) TOA reflectance to surface reflectance, 15% of the observations with the minimum blue surface reflectance were identified as “clearest” ones. To avoid cloud-shadows, the observations with blue reflectance smaller than 0.01 were excluded. There are four AERONET sites with the measured optical depth data in this local area during this period of time: Goddard Space Flight Center (GSFC) at Greenbelt, Maryland (39.03°N, 76.88°W); Smithsonian Environmental Research Center (SERC) at Annapolis, Maryland (38.88°N, 76.50°W); Maryland Science Center at Baltimore, Maryland (39.28°N, 76.61°W); and Wallops Island, Virginia (37.94°N, 75.47°W). The estimated aerosol optical depths of blue band (band 3) using the new algorithm are compared with AERONET measurements and shown in Fig. 3. Both are in great agreement. We do see some points whose aerosol optical depth is smaller than the threshold of 0.07 from AERONET observations, which indicates that this new algorithm cannot deal well with these situations. The MODIS aerosol product

(MOD04) that has the spatial resolution of 10km\*10km is also compared with the AERONET measurements in the same figure. Although their spatial resolutions are different, it is not difficult to conclude that our new algorithm works more effectively than the MODIS algorithm for estimating aerosol optical depth over non-vegetated surfaces. At the Wallops Island site, MOD04 does not even have a clear trend correlated with the AERONET measurements. Note that the number of the points of two plots at each site is different because there are no retrievals on many dates in the MOD04 product. Keep in mind that we always expect some differences between the retrieved values from MODIS data and the AERONET measurements because of the scale mismatch among the AERONET “point” measurements, 1 km resolution from the new algorithm and 10 km from MOD04 product.

The second case is over Beijing, China, where 166 MODIS images were selected from October 1, 2002 to December 31, 2002 and 377 MODIS images were chosen from September 1, 2003 to April 1, 2004. The landscape of Beijing during these two periods is mostly non-vegetated surfaces. The parameters in the algorithm used in this case are the same as those used with data over the greater Washington, DC area. The retrieved results using this algorithm and the MODIS aerosol product (MOD04) are compared with the AERONET observations in Fig. 4. The new algorithm performs very well, but there are large scattering in the validation results of the MOD04 product.

Fig. 5 shows the color-composite image of the MODIS observations acquired on November 11, 2002, which is very hazy and most likely covered by dust and other aerosols. The spatial resolution of the image is 1 km. The MODIS data were ordered from DAAC. The spatial distribution of the retrieved aerosol optical depth is shown in Fig. 6. Visually, the retrieved aerosol optical depths match the spatial patterns

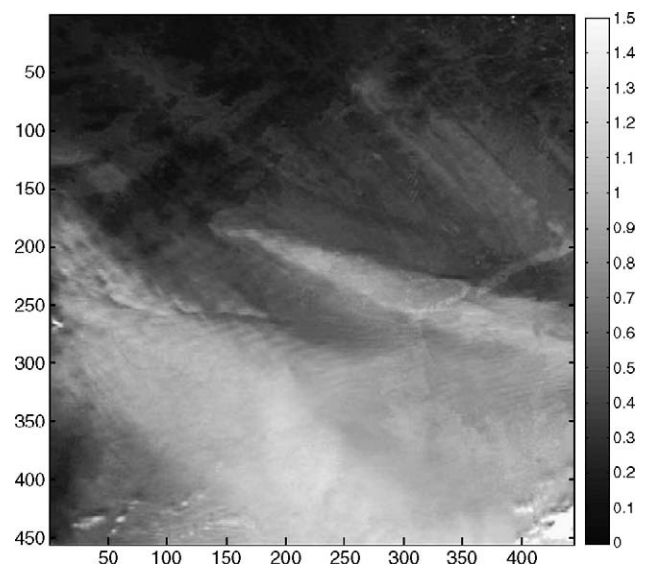


Fig. 6. The retrieved aerosol optical depth of blue band from the image in Fig. 4 using the new algorithm.

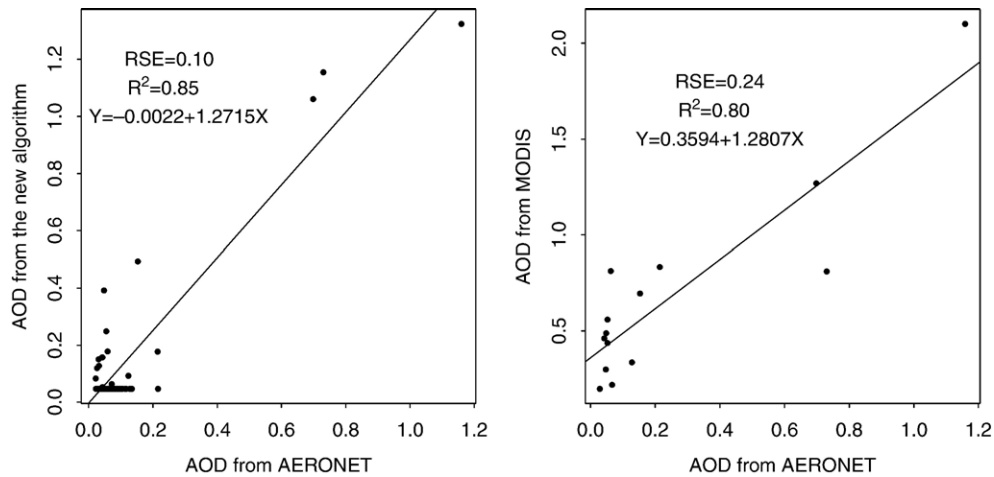


Fig. 7. Validation results using AERONET measurements at Bratts Lake, Canada. The left plot is for validating the new algorithm and the right plot is for the MOD04 product. The solid line is the regression line and the regression equation is also given in each plot. The aerosol optical thickness (AOT) corresponds to MODIS blue band (band 3).

of the hazy imagery very well. Note that there are clouds in this image and the cloudy pixels were inverted in the same way as the hazy pixels. There is no reason to believe that the retrieved optical depths of the cloudy pixels are accurate, but we retain those pixels in the image for visualization purposes.

The third case is in the area of Bratts Lake, Canada. This AERONET instrument is located at Bratt's Lake on the prairies (50.28°N, 104.70°W) with an elevation of 586.7m. Winter is long in this area and snow is the main land cover during winter. We downloaded 414 MODIS images from September 1, 2003 to April 1, 2004. Fig. 7 shows the validation results at this site.

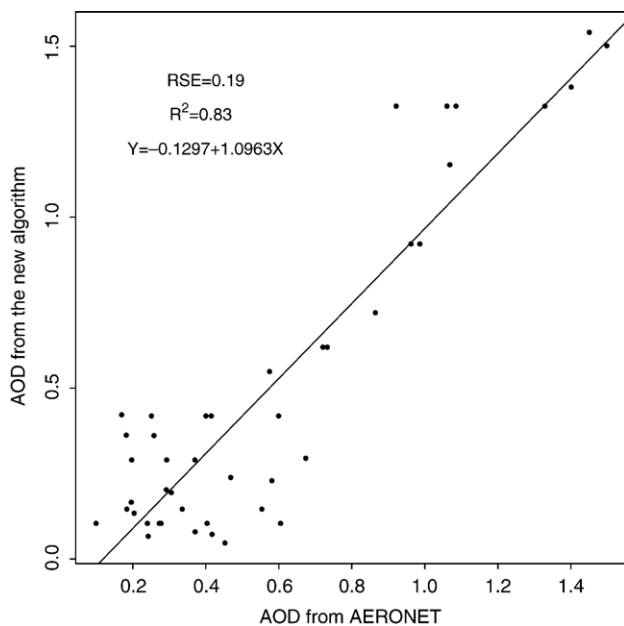


Fig. 8. Validation results using AERONET measurements at Niger, Africa. The solid line is the regression line and the regression equation is also given in each plot. The aerosol optical thickness (AOT) corresponds to MODIS blue band (band 3).

Both algorithms perform reasonably well, but both plots show large scattering.

The fourth case is over Banizoumbou, Niger, Africa. This site is located on a small isolated plateau in a cultivated sandy area near the village of Banizoumbou, 60km east of Niamey. There is an AERONET site located at 13.54°N, 2.66°E. The surface elevation is 250m. We ordered 304 MODIS images from September 1, 2003 to April 1, 2004. The procedure and the parameters are the same as those at the other test sites. The only difference is that a much larger aerosol optical depth (0.4 in the blue band) was used for the “clearest” atmosphere, instead of 0.07 used in other cases, because the atmosphere is quite “turbid” even if it is a clear day in this region. The validation results for the new algorithm are shown in Fig. 8. Clearly, there is a good linear correlation overall, but the scattering is larger and this new algorithm does not perform as well as we might expect when the atmosphere is clear. It is partially due to the threshold value we used. Characterization of surface and aerosol properties may also affect this pattern. However, the MOD04 imagery is full of filled values and inadequate points could be used for comparison.

Fig. 9 shows the combined validation results from all the sites. It is clear that the residual standard errors and  $R^2$  values of the new method are much better than the MOD04 product. The retrievals from this new algorithm are not biased, but the MOD04 product seems significantly underestimated.

There are two important issues in this procedure. The first is to determine the surface reflectance using the “clearest” blue-band apparent surface reflectance, and the second is to characterize the aerosol models. In the follow-up study (Zhong et al., submitted for publication), we have addressed both issues by applying this approach to the MODIS data at 25 AERONET sites over North America where the detailed aerosol parameters (e.g., optical depth, aerosol model) are retrieved from the AERONET measurements. It is found that this

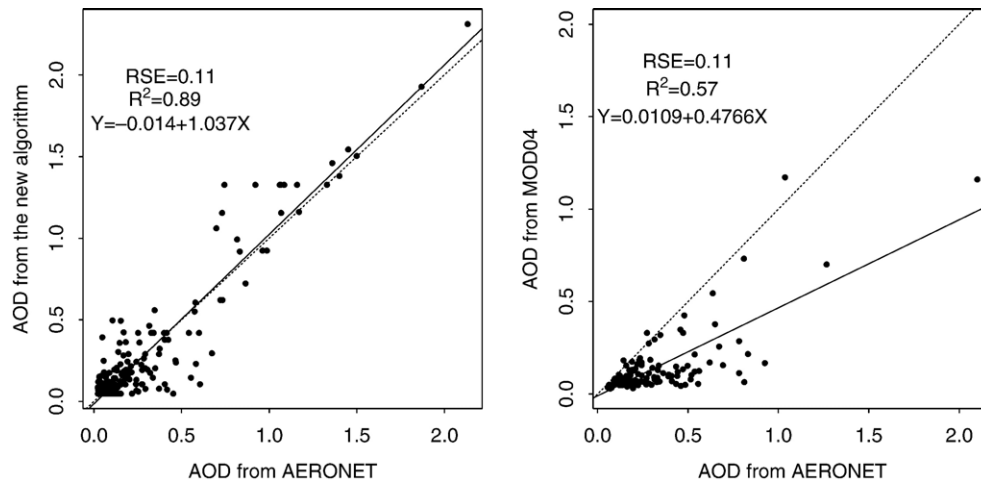


Fig. 9. Combined validation results using AERONET measurements from all sites shown in the previous figures where the dash lines are 1:1 lines and the solid lines are regression lines. The left plot is for validating the new algorithm and the right plot is for the MOD04 product. The regression equation is also given in each plot. The aerosol optical thickness (AOT) corresponds to MODIS blue band (band 3).

procedure is mostly sensitive to the determination of surface reflectance and the impact of the aerosol model selection is secondary. We found that 15% of the observations provide us with the best retrieval. For reference, the determined surface blue-band reflectances at these validation sites are summarized in Table 1.

## 5. Summary and conclusions

In this study, we have developed a new algorithm for estimating aerosol optical depth from MODIS data suitable for all land surfaces. This algorithm is based on a sequence of imagery within a period of time with the assumption that surface property is relatively stable and atmospheric conditions vary dramatically. Four case studies at four different regions of the world have demonstrated that this new algorithm can retrieve aerosol optical depths from MODIS imagery over non-vegetated (“bright”) surfaces within a reasonable agreement with the AERONET measured values, where the MODIS aerosol estimation algorithm is unable to accurately capture the tremendous amount of variations in aerosol optical depth because the MODIS algorithm relies on the presence of dense vegetation on the surface. Compared to the AERONET measurements, the residual standard error and  $R^2$  values of the new algorithm are 0.11 and 0.89, while the

corresponding values of the MOD04 product are 0.11 and 0.57.

More extensive experiments and validations are still needed to determine the relevant parameters (e. g., the length of the temporal window, optical depth of the clearest observations) under different conditions for a global implementation. Particular attentions should be paid to rapid surface changes (e.g., raining/snowing, flooding) and the deliberate incorporation of more realistic surface BRDF at the kilometer scale.

In retrieving aerosol optical depths, the look-up table approach has been used in this study. To create and search the look-up tables, one has to pre-define the aerosol models for a given time and space, as is done in the current MODIS algorithm. Unfortunately, selecting different aerosol models has been found to have a profound impact on the final retrieval. There is an urgent need for developing the aerosol model climatology at a fine spatial and temporal resolution from satellite products (e.g., MISR), ground measurements (e.g., AERONET) and/or their combinations.

The basic requirement of this new method for satellite imagery is the high temporal resolution (say, daily). This requirement is not a limiting factor for most moderate spatial resolution sensors, such as Medium-Resolution Imaging Spectrometer (MERIS), Sea-viewing Wide Field-of-view Sensor (SeaWiFS), Advanced Very High Resolution Radiometer (AVHRR) and Global Imager (GLI). Therefore, this approach can be potentially useful for the images of those satellite sensors.

Table 1  
Statistics of the retrieved surface blue-band reflectance of the “clear” pixels

Validation sites	Mean	Standard deviation
GSFC	0.0666	0.00628
MD Science Center	0.0490	0.00065
SERC	0.0248	0.00012
Wallops	0.0370	0.00035
Beijing	0.1056	0.00185
Banizoumbou	0.0826	0.00015
Bratts Lake	0.0528	0.00194

## Acknowledgment

The authors are very grateful to Dr. Brent Holben at the NASA Goddard Space Flight Center for making AERONET data available to the public through the Internet, and anonymous reviewers for their thoughtful comments, which have greatly improved the presentation of this paper.

## References

- Chavez, J. P. (1996). Image-based atmospheric corrections—revisited and improved. *Photogrammetric Engineering and Remote Sensing*, 62, 1025–1036.
- Christopher, S. A., Zhang, J., Holben, B. N., & Yang, S. K. (2002). Goes-8 and NOAA-14 AVHRR retrieval of smoke aerosol optical thickness during scarb. *International Journal of Remote Sensing*, 23, 4931–4944.
- Deuze, J. L., Breon, F. M., Devaux, C., Goloub, P., Herman, M., Lafrance, B., et al. (2001). Remote sensing of aerosols over land surfaces from polder-aerosol-1 polarized measurements. *Journal of Geophysical Research - Atmosphere*, 106, 4913–4926.
- Diner, D. J., Martonchik, J. V., Kahn, R. A., Pinty, B., Gobron, N., Nelson, D. L., et al. (2005). Using angular and spectral shape similarity constraints to improve MISR aerosol and surface retrievals over land. *Remote Sensing of Environment*, 94, 155–171.
- Fallah-Adl, H., JaJa, J., & Liang, S. (1997). Fast algorithms for estimating aerosol optical depth of thematic mapper (TM) imagery. *Journal of Supercomputing*, 10, 315–330.
- Hall, F. G., Strelbel, D. E., Nickeson, J. E., & Goetz, S. J. (1991). Radiometric rectification: Toward a common radiometric response among multitemporal, multisensor images. *Remote Sensing of Environment*, 35, 11–27.
- Hapke, B. (1984). Bidirectional reflectance spectroscopy. 3. Correction for macroscopic roughness. *Icarus*, 59, 41–59.
- Hauser, A., Oesch, D., Foppa, N., & Wunderle, S. (2005). NOAA AVHRR derived aerosol optical depth over land. *Journal of Geophysical Research - Atmospheres*, 110.
- Herman, J. R., Celarier, E., & Larko, D. (2001). UV 380nm reflectivity of the earth's surface, clouds and aerosols. *Journal of Geophysical Research*, 106, 5335–5351.
- Holben, B. N. (1986). Characteristics of maximum-value composite images for temporal AVHRR data. *International Journal of Remote Sensing*, 7, 1435–1445.
- Holben, B. N., Eck, T., Slutsker, I., Tanre, T., Buis, J., Setzer, A., et al. (1998). Aeronet—a federated instrument network and data archive for aerosol characterization. *Remote Sensing of Environment*, 66, 1–16.
- Hsu, N. C., Tsay, S. C., King, M. D., & Herman, J. R. (2004). Aerosol properties over bright-reflecting source regions. *IEEE Transactions on Geoscience and Remote Sensing*, 42, 557–569.
- Kaufman, Y. J., Karnieli, A., & Tanre, D. (2000). Detection of dust over deserts using satellite data in the solar wavelengths. *IEEE Transactions on Geoscience and Remote Sensing*, 38, 525–531.
- Kaufman, Y. J., Tanre, D., & Boucher, O. (2002). A satellite view of aerosols in the climate system. *Nature*, 419, 215–223.
- Kaufman, Y. J., Tanre, D., Gordon, H. R., Nakajima, T., Lenoble, J., Frouin, R., et al. (1997a). Passive remote sensing of tropospheric aerosol and atmospheric correction for the aerosol effect. *Journal of Geophysical Research*, 102(D14), 16815–16830.
- Kaufman, Y. J., Tanre, D., Remer, L., Vermote, E. F., Chu, A., & Holben, B. N. (1997b). Operational remote sensing of tropospheric aerosol over the land from EOS-MODIS. *Journal of Geophysical Research*, 102, 17051–17068.
- Kaufman, Y. J., Wald, A., Lorraine, L. A., Gao, B. C., Li, R. R., & Flynn, L. (1997c). Remote sensing of aerosol over the continents with the aid of a 2.2 $\mu$ m channel. *IEEE Transactions on Geoscience and Remote Sensing*, 35, 1286–1298.
- Levy, R. C., Remer, L. A., Martins, J. V., Kaufman, Y. J., Plana-Fattori, A., Redemann, J., et al. (2005). Evaluation of the MODIS aerosol retrievals over ocean and land during clams. *Journal of the Atmospheric Sciences*, 62, 974–992.
- Liang, S. (2004). *Quantitative remote sensing of land surfaces* (pp. 534). John Wiley and Sons, Inc.
- Liang, S., Fallah-Adl, H., Kalluri, S., JaJa, J., Kaufman, Y. J., & Townshend, J. R. G. (1997). An operational atmospheric correction algorithm for landsat thematic mapper imagery over the land. *Journal of Geophysical Research - Atmosphere*, 102, 17173–17186.
- Liang, S., & Fang, H. (2004). An improved atmospheric correction algorithm for hyperspectral remotely sensed imagery. *IEEE Geoscience and Remote Sensing Letters*, 1, 112–117.
- Liang, S., Fang, H., & Chen, M. (2001). Atmospheric correction of landsat ETM + land surface imagery: I. Methods. *IEEE Transactions on Geoscience and Remote Sensing*, 39, 2490–2498.
- Liang, S., & Townshend, J. (1997). Angular signatures of NASA/NOAA Pathfinder AVHRR Land data and applications to land cover identification. *Proceedings of IGARSS*, 4, 1781–1783.
- Martonchik, J. V., Diner, D. J., Crean, K. A., & Bull, M. A. (2002). Regional aerosol retrieval results from MISR. *IEEE Transactions on Geoscience and Remote Sensing*, 40, 1520–1531.
- Martonchik, J. V., Diner, D. J., Kahn, R. A., Ackerman, T. P., Verstraete, M. E., Pinty, B., et al. (1998). Techniques for the retrieval of aerosol properties over land and ocean using multiangle imaging. *IEEE Transactions on Geoscience and Remote Sensing*, 36, 1212–1227.
- Moran, M. S., Jackson, R. D., Slater, P. N., & Teillet, P. M. (1992). Evaluation of simplified procedures for retrieval of land surface reflectance factors from satellite sensor output. *Remote Sensing of Environment*, 41, 169–184.
- North, P. R. J. (2002). Estimation of aerosol opacity and land surface bidirectional reflectance from atsr-2 dual-angle imagery: Operational method and validation. *Journal of Geophysical Research - Atmosphere*, 107 (Article no. 4149).
- Popp, T. (1995). Correcting atmospheric masking to retrieve the spectral albedo of land surface from satellite measurements. *International Journal of Remote Sensing*, 16, 3483–3508.
- Qin, W., Herman, J. R., & Ahman, Z. (2001). A fast, accurate algorithm to account for non-lambertian surface effects on TOA radiance. *Journal of Geophysical Research*, 106, 22671–22684.
- Remer, L. A., Kaufman, Y. J., Tanre, D., Mattoo, S., Chu, D. A., Martins, J. V., et al. (2005). The MODIS aerosol algorithm, products, and validation. *Journal of the Atmospheric Sciences*, 62, 947–973.
- Salomonson, V., Barnes, W., Maymon, P., Montgomery, H., & Ostrow, H. (1989). MODIS: Advanced facility instrument for studies of the earth as a system. *IEEE Transactions on Geoscience and Remote Sensing*, 27, 145–153.
- Tang, J., Xue, Y., Yuc, T., & Guan, Y. N. (2005). Aerosol optical thickness determination by exploiting the synergy of Terra and Aqua MODIS. *Remote Sensing of Environment*, 94, 327–334.
- Teillet, P. M., & Fedosejevs, G. (1995). On the dark target approach to atmospheric correction of remotely sensed data. *Canadian Journal of Remote Sensing*, 21, 374–387.
- Torres, O., Bhartia, P. K., Herman, J. R., Sinyuk, A., Ginoux, P., & Holben, B. (2002). A long-term record of aerosol optical depth from TOMS observations and comparison to AERONET measurements. *Journal of the Atmospheric Sciences*, 59, 398–413.
- Tripathi, S. N., Dey, S., Chandel, A., Srivastava, S., Singh, R. P., & Holben, B. N. (2005). Comparison of MODIS and AERONET derived aerosol optical depth over the Ganga basin, India. *Annales Geophysicae*, 23, 1093–1101.
- Walthall, C. L., Norman, J. M., Welles, J. M., Campbell, G., & Blad, B. L. (1985). Simple equation to approximate the bi-directional reflectance from vegetation canopies and bare soil surfaces. *Applied Optics*, 24, 383–387.
- Wang, J., Christopher, S. A., Reid, J. S., Maring, H., Savoie, D., Holben, B. N., et al. (2003). GOES 8 retrieval of dust aerosol optical thickness over the Atlantic Ocean during pride. *Journal of Geophysical Research*, 108 (Art. No. 8595).
- Zhang, J., & Christopher, S. A. (2001). Intercomparison of smoke aerosol optical thickness derived from GOES 8 imager and ground-based sun photometers. *Journal of Geophysical Research*, 106, 7387–7397.
- Zhong, B., Liang, S., & Holben, B. (submitted for publication). Validation of a new algorithm for estimating aerosol optical depth from MODIS imagery. *International Journal of Remote Sensing*.